

ON THE CLOSE ENCOUNTERS BETWEEN PLUTINOS AND NEPTUNE TROJANS:
II. RANDOM WALK AND AGGREGATE EFFECT

DONG CHENG-YU¹ AND ZHOU LI-YONG^{1,2,*}

¹*School of Astronomy and Space Science, Nanjing University, Nanjing 210046, China*

²*Key Laboratory of Modern Astronomy and Astrophysics in Ministry of Education, Nanjing University, Nanjing 210046, China*

ABSTRACT

In the previous paper, we conducted detailed statistical analyses on the geometry and dynamic effect of the close encounters between Plutinos and Trojans, and concluded that the close encounter is a random and unbiased process. However, the random walk theory will drive impartial effect to gradually accumulate given sufficient times. Based on the analytical formula derived in the previous paper, we theoretically explore the cumulative effect of close encounters contributed by one Plutino and a group of Plutinos, and find that the effect drops reciprocally as the number of Plutinos that share fixed total mass increases. After testing this theoretical approach against possibly involved parameters one by one, we generalize it to arbitrary Plutino or Trojan, whereby the cumulative effect of groups of different planetesimals can now be theoretically estimated. As a result, the realistic effect is believed to be insignificant. Nevertheless, we further find that a Plutino with sufficient mass will expel Trojan from its resonance region. By means of a mixed strategy, we build an intensity factor to well explain this phenomenon, and it can be applied to groups of planetesimals as well.

Keywords: celestial mechanics — Kuiper belt: general — methods: miscellaneous — minor planets, asteroids: general

* zhouly@nju.edu.cn

1. INTRODUCTION

Neptune Trojans are minor objects dynamically trapped in the 1:1 mean motion resonance (MMR) with Neptune, and spatially situated in the vicinities of L_4 and L_5 , namely the Lagrange points ahead of and behind Neptune respectively. Since the first discovered Neptune Trojan 2001QR322 (Pittichova et al. 2003), a few more were discovered¹, more than half of which possess high inclinations. The stability and origin of highly inclined Neptune Trojans have been widely studied (Marzari et al. 2003; Dvorak et al. 2007, 2008; Zhou et al. 2009; Brasser et al. 2004; Li et al. 2007), but yet not able to be fully explained.

In the previous paper (Dong & Zhou 2017, hereafter Paper I), along with the idea of Almeida et al. (2009), we conceive that the close encounters (CEs) brought by Plutinos may serve as a persistent mechanism to elevate the inclinations of Trojans. To address that, we implement numerical simulations to capture the CE information of four typical pairs of Plutinos and Trojans, as well as statistical analyses on the feature variables associated with CE locations and CE effects. Though different from one to another in the specific distributions, all four pairs are found to produce impartial CEs, indicating a purely random process. The further applied Monte Carlo (M-C) simulations obtain nearly the same statistical diagrams of pertinent variables as the numerical simulations, which again verify the above conclusion.

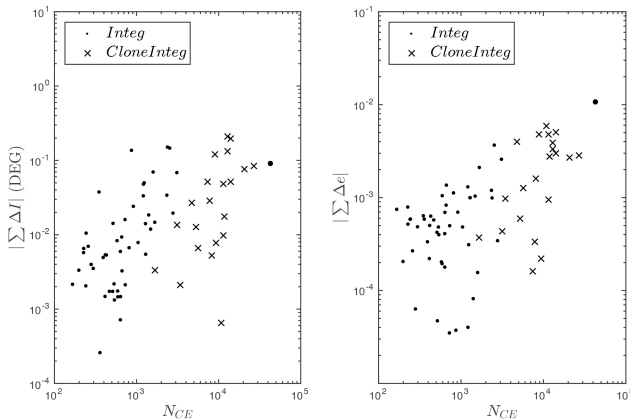


Figure 1. $|A_I|$ ($|A_e|$), the absolute value of arithmetic sum of ΔI (Δe), relates to N_{CE} , the number of CE. “•” comes from a direct numerical simulation between one real Trojan and several real Plutinos. “×” comes from the numerical simulation between one Trojan and several clones of Plutinos in order to raise the number of CEs. The specific method to clone is mentioned in the previous paper. The big “•” residing at a very large N_{CE} denotes the sum of all ΔI (Δe) from “•”.

¹ IAU: Minor Planet Center, <http://www.minorplanetcenter.net/iau/lists/NeptuneTrojans.html>

Intuitively, a random process is impossible to bring about evident cumulative effect, for the positive and negative effect ought to cancel each other out only if given considerably long time. However, by summarizing the so far obtained CE effect data from numerical simulations, we end up to get a dramatically opposite result. Let

$$A_I \equiv \sum_{i=1}^{N_{CE}} \Delta I_i, \quad A_e \equiv \sum_{i=1}^{N_{CE}} \Delta e_i, \quad (1)$$

which are the arithmetic sums of all the inclination changes or eccentricity changes during CE in a specific simulation. Fig. 1 shows $|A_I|$ or $|A_e|$ with respective to the number of CEs for different simulations. One can easily find out a positive correlation in a logarithmic scale, which indicates that the cumulative effect will increase significantly as more CE happens. This correlation is certainly not a transient state in the simulation and tends to be a statistical property.

We now introduce the theory of random walk, which is a statistical model primordially originating from the irregular motion of a pollen, later known as Brownian motion. In precedent works, the random walk theory is frequently applied to recurrent processes, such as the close encounters with Vesta in the main belt (Carruba et al. 2007), and non-destructive collisions (Dell’Oro & Cellino 2007). As suggested by Fig. 1, in this work we will implement the random walk theory to theoretically study the cumulative effect of CEs, namely A_I and A_e . Of course the arithmetic sums of change of orbital elements during CEs are unlikely to be the precise variations after such CEs, since the dynamic system with multi-body interactions is chaotic and unpredictable, but at least it can offer an order of magnitude approximately.

The detailed introduction to random walk and associated applications will be embodied in Sect. 2, where we combine the analytical approximation on the number of CEs, and the theoretical distribution of CE effect mentioned in Paper I, to give a acceptable estimation on the cumulative effect. Then in Sect. 3, we build a new algorithm to address the potential escape of Trojan from the resonant region. Main results and inspirations will be discussed in Sect. 4.

2. RANDOM WALK AND THE CUMULATIVE EFFECT

We now aim to analytically express $A_I(A_e)$, namely the cumulative effect of orbital elements change after a number of CEs. This problem can actually be fitted into a one-dimensional random walk with a varying step size. The inclination of Trojan either increases or decreases at a equal chance but with different absolute value of inclination change in each step according to the relative distance and other factors. The order of magnitude of entire inclination variation is able to be anticipated using a particular random walk theory. This also applies to the eccentricity.

2.1. One-dimensional Gaussian random walk

A Gaussian random walk has a step size that varies according to a normal distribution, namely

$$X \sim N(\mu, \sigma^2). \quad (2)$$

The sum of n steps with identical distribution can be expressed as

$$Z = \sum_{i=1}^n X_i, \quad (3)$$

which obeys

$$Z \sim N(n\mu, n\sigma^2). \quad (4)$$

For the special case where $\mu = 0$,

$$Z \sim N(0, n\sigma^2). \quad (5)$$

Thereupon mathematical expectation of the absolute value of this sum is

$$E(|Z|) = \sqrt{\frac{2}{\pi}} \sigma \sqrt{n} \quad (6)$$

As for our model, since the close encounters have qualified as a random process, ΔI (Δe), namely the effect in each CE can be treated as a random variable with a specific probability distribution. If that distribution happens to be Gaussian, the cumulative variation of orbital element A_I (A_e) will then obey a Gaussian distribution, and the mathematical expectation of its absolute value can be estimated based on Eq. (6), given the standard deviation σ and number of CEs n . The term $\mu = 0$ is naturally satisfied since we have proven the impartiality of CE effect in Paper I.

Now by reference to Paper I, it can be easily recognized that the distribution of ΔI (Δe) is far from a standard Gaussian profile. Nevertheless, the central limit theorem (CLT), written as

$$\frac{Z - n\mu}{\sqrt{n}\sigma} \sim N(0, 1), \quad n \rightarrow \infty, \quad (7)$$

fortunately shows that as long as there are sufficient CEs, the cumulative effect will always approach a Gaussian profile, regardless of the specific distribution of each step. In other words, Eq. 6 remains applicable.

2.2. Fitting and verification

Now we can see if the simulation results conform to the random walk theory. Consider that ΔI in one CE is a random variable with a probability density function $f(\Delta I)$, mathematical expectation $\mu_I = 0$ and standard deviation σ_I . Assuming ΔI to be independent and identically distributed in all CEs, we have

$$A_I \sim N(0, N_{CE} \sigma_I^2), \quad (8)$$

where N_{CE} is the number of CEs and thus

$$E(|A_I|) = \sqrt{\frac{2}{\pi}} \sigma_I \sqrt{N_{CE}}. \quad (9)$$

Given a sample of CE effect data, σ_I can be estimated by a sample standard deviation, yielding

$$s_I \equiv \sqrt{\frac{1}{N_{CE} - 1} \sum_{i=1}^{N_{CE}} (\Delta I_i - \bar{\Delta I})^2}, \quad (10)$$

which is not an unbiased estimator for the population standard deviation, though generally used if given enough sample points. Hence Eq. (9) can be rewritten as

$$E(|A_I|) = \sqrt{\frac{2}{\pi} \frac{N_{CE}}{N_{CE} - 1} \sum_{i=1}^{N_{CE}} (\Delta I_i - \bar{\Delta I})^2}, \quad (11)$$

which is useful to directly analyze the CE data generated through a simulation.

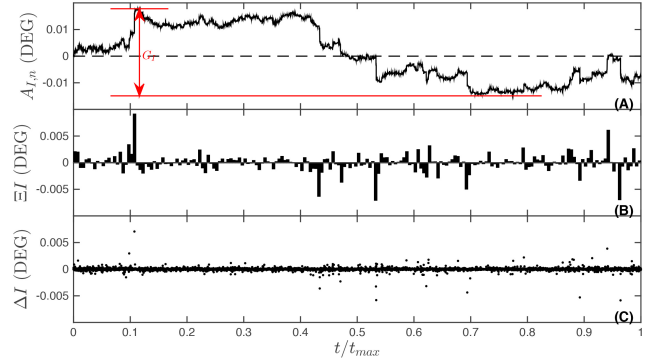


Figure 2. The illustration for random walk range G_I and some other statistics. (A): The arithmetic sum of all the ΔI before current time, namely $A_{I,n} = \sum_{i=1}^n \Delta I_i$, versus time ratio. (B): The sum of all the ΔI within a specified time interval. (C): ΔI

Define

$$G_I = \max_{1 \leq n \leq N_{CE}} \sum_{i=1}^n \Delta I_i - \min_{1 \leq n \leq N_{CE}} \sum_{i=1}^n \Delta I_i, \quad (12)$$

which is the maximum inclination variation ever accumulated, also known as the range of random walk. According to the expression, we may intuitively imagine that the expectation of G_I should be two times the expectation of A_I , whereas we are not going to prove it here, since G_I merely serves as a test statistic not that significant in the following discussion. We may tentatively write

$$E(|G_I|) = 2 \sqrt{\frac{2}{\pi}} \sigma_I \sqrt{N_{CE}}. \quad (13)$$

Substituting σ_I by the sample estimator s_I , we have

$$E(|G_I|) = 2 \sqrt{\frac{2}{\pi} \frac{N_{CE}}{N_{CE} - 1} \sum_{i=1}^{N_{CE}} (\Delta I_i - \bar{\Delta I})^2}. \quad (14)$$

The above theory can be equivalently applied to the CE effect on the eccentricity. Therefore we have

$$E(|A_e|) = \sqrt{\frac{2}{\pi} \frac{N_{CE}}{N_{CE} - 1} \sum_{i=1}^{N_{CE}} (\Delta e_i - \bar{\Delta e})^2}, \quad (15)$$

and

$$E(|G_e|) = 2 \sqrt{\frac{2}{\pi} \frac{N_{CE}}{N_{CE} - 1} \sum_{i=1}^{N_{CE}} (\Delta e_i - \bar{\Delta}e)^2}. \quad (16)$$

Fig. 3 (A,B) shows a direct comparison between the theoretical expectation (filled symbols) and the experimental value (open symbols) of $|A_I|$ ($|A_e|$) from a bunch of numerical simulations and M-C simulations. A vertical line segment links the filled dot to the corresponding outlined dot to show the difference. On (A), basically, the theory goes well, except for data coming from M-C method (“ Δ ”), and the difference is more prominent on (A2). This may be derived from the relative error of M-C method, which is more significant for eccentricity as mentioned in Paper I. On (B), the theory fits really fine, with the theoretical value almost overlapping the experimental value, probably because the subtraction from maximum sum to minimum ought to eliminate the transient effect in random walk to some degree.

On Fig. 3 (C), s_I (s_e) is denoted for each simulation, basically unchanged for the same pair of interacting particles, which supports our assertion in Sect. 2.1. Thereupon if we believe all CE effect data for the same pair, no matter from numerical integration or M-C method, are taken from an identical population, we can combine them into one sample and obtain \bar{s}_I (\bar{s}_e), a more precise estimator for σ_I (σ_e), which is denoted by a horizontal line in Fig. 3 (B). Using this aggregated sample standard deviation, a theoretical curve can then be plotted on Fig. 3 (A,B), according to Eq. (9) and Eq. (13), which will contain only one undetermined variable N_{CE} . Therefore, for a specific pair, $|A_I|$ can be estimated simply by N_{CE} . For example, Plutino 1999CE119 can shift the inclination of Trojan 2004UP10 for more than 0.3 degree after 1×10^5 CEs approximately².

2.3. The theoretical estimation on the cumulative effect

In this section we try to theoretically explore the cumulative CE effect on the orbital elements of Trojan. Specifically, we need to derive the expression for the magnitude of A_I and A_e defined above.

2.3.1. The theoretical number of CEs

The general expression for the number of CEs obviously serves as a prerequisite for the discussion on the cumulative effect, while in fact, this problem is equivalent to solving the collision probability between two planetesimals given their orbits elements. A number of precedent works focused on this classical topic, such as Wetherill (1967) and Greenberg (1982), which both derived accurate formulas through complex geometrical relationships given a fixed pair of orbital elements. However, due to the complicated secular evolutions of orbital elements in resonances, we decide to develop our

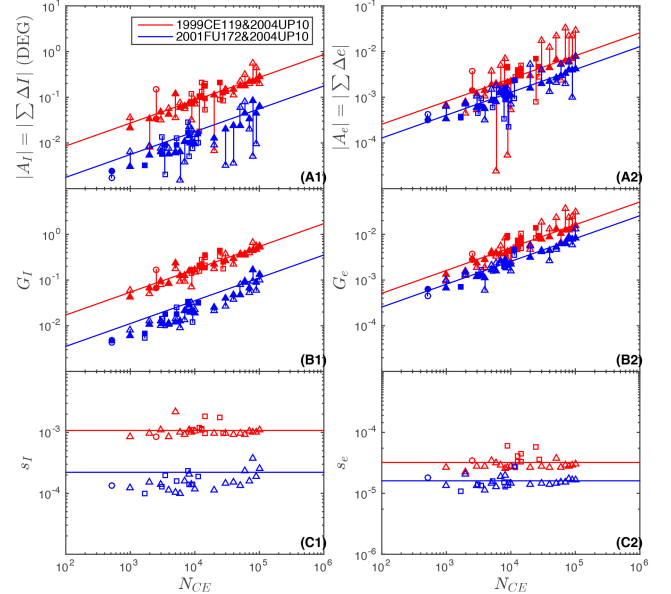


Figure 3. (A): $|A_I|$ ($|A_e|$) versus N_{CE} in a logarithmic scale. (B): G_I (G_e) versus N_{CE} in a logarithmic scale. (C): s_I (s_e) versus N_{CE} in a logarithmic scale. In each plot, “o” comes from a numerical simulation between 2004UP10 and 1999CE119 (Blue) or 2001FU172 (Red). “□” comes from the numerical simulation between 2004UP10 and several clones of 1999CE119 (Blue) or 2001FU172 (Red). “ Δ ” comes from the M-C simulation between 2004UP10 and 1999CE119 (Blue) or 2001FU172 (Red). The different types of filled dots represent the expected $|A_I|$ calculated by Eq. (11) corresponding to different types of dots respectively. A vertical line segment is drawn between the experimental value and theoretical value to show the difference. On the left, the fitting curves on (A1) and (B1) denote $|A_I| = \sqrt{2/\pi} \bar{s}_I \sqrt{N_{CE}}$ and $G_I = 2 \sqrt{2/\pi} \bar{s}_I \sqrt{N_{CE}}$ respectively, where \bar{s}_I is the aggregated estimator for σ_I from all samples for this pair, located at the horizontal line on (C1). This goes the same way on the right. The M-C simulation is introduced here in order to give multiple instances as supplements for numerical simulations.

own analytical approximation on N_{CE} , which may be rough, but comprehensible.

Recall the probability of a CE locating within a specific radius in Paper I, namely

$$P(\tilde{R} < R) = \left(\frac{R}{R_{th}} \right)^2, \quad (17)$$

which can be easily understood in a “cross section” sense. Now if we presumably extend this correlation to a much large region with scale length $R_U \gg R_{th}$, the number of CEs within R_{th} can be deduced given the total number of potential encounters, namely

$$N_{CE} = N_U \left(\frac{R_{th}}{R_U} \right)^2. \quad (18)$$

² Note that the Plutino has an hypothetical Pluto mass, which is far from the real case.

We now have to quantify N_U and R_U in Eq. (18). Considering the total time in simulations is 1Gyr, along with the fact that Plutino tends to meet Trojan every two laps since Plutino and Trojan are trapped in 2:3 and 1:1 resonances with Neptune respectively, the total number of potential encounters can be written as

$$N_U = \frac{t_{tot}}{2t_{orb}} = \frac{t_{tot}/\text{yr}}{2(a_P/\text{AU})^{3/2}}. \quad (19)$$

Next, since the encounter comes up only when Plutino approaches the orbit of Trojan, a rectangular region can be roughly defined around the overlap between the orbits of the two, as shown in Fig. 4. Concretely, we approximately put the orbits of Plutino and Trojan onto the same plane and omit the eccentricity of Trojan, indicating kinds of average case between orbits crossing at the perihelion and aphelion of Trojan. The distance between the two intersections can thus be regarded as half the width of the encounter region. Therefore we have a set of equation

$$\begin{aligned} a_P^2 &= (x + a_P e_P)^2 + \frac{y^2}{1 - e_P^2}, \\ a_T^2 &= x^2 + y^2, \end{aligned} \quad (20)$$

from which y can be solved and the width $W = 4y$.

Meanwhile, the length can be roughly regarded as two times the extent that the perihelion of Plutino stretches into the orbit of Trojan, namely

$$L = |a_P(1 - e_P) - a_T(1 - e_T)| + |a_P(1 - e_P) - a_T(1 + e_T)|, \quad (21)$$

where we take the average of the perihelion and aphelion cases.

Finally, the height is naturally the vertical gap between the summits of the two orbits. Considering the one side or two sides case, a simple geometric mean gives

$$H = 2a_P(1 - e_P) \sqrt{\sin(I_P + I_T) \sin|I_P - I_T|} \quad (22)$$

Note that Fig. 4 shows a completely hypothetical circumstance where the directions of the semi-axes of Plutino and Trojan overlaps each other, based on which we are able to give the above derivations. Though be unrealistic, the combination of L , W and H at least gives a coarse estimation for the size of the encounter region, from which the scale length R_U can be derived as

$$R_U = \left(\frac{4\pi}{3} L \cdot W \cdot H \right)^{1/3}. \quad (23)$$

Together with Eq. (19), (23) and the expression for CE threshold³

$$R_{th} = \kappa_{th} a_P \left(\frac{m_P}{3m_S} \right)^{1/3}, \quad (24)$$

³ This expression for Hill radius is same as what we use in the numerical simulation. $\kappa_{th} = 3.5$ as previously mentioned.

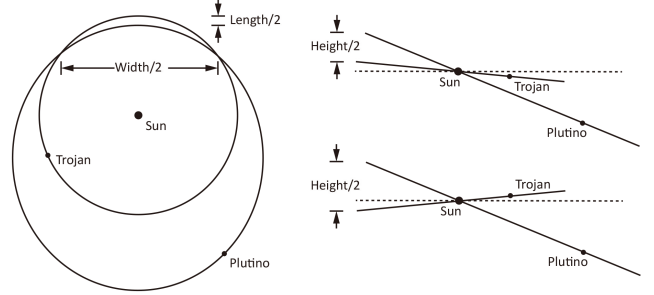


Figure 4. The face-on and edge-on projections of the encounter region. The length is roughly the extent that the orbit of Plutino stretches into that of Trojan. The width is the distance between the intersections of the projections of the orbits while the height is the vertical distance between the perihelia of Plutino and Trojan. Note that there are two types of heights according to the relative locations of the orbits.

we finally obtain the specific correlation between N_{CE} and m_P , namely

$$N_{CE} = \chi_N v_P^{2/3}, \quad (25)$$

where

$$\chi_N = \left(\frac{\kappa_{th} a_P}{R_u} \right)^2 \left(\frac{v_{Pluto}}{3} \right)^{2/3}, \quad (26)$$

$$v_P \equiv \frac{m_P}{m_{Pluto}}, \quad (27)$$

and

$$R_u \equiv \frac{R_U}{\sqrt{N_U}}, \quad (28)$$

$$v_{Pluto} \equiv \frac{m_{Pluto}}{m_S}. \quad (29)$$

We have scaled m_P with Pluto mass here.

2.3.2. The cumulative effect

Now that we have the analytical expression for N_{CE} , A_I seems easy to derive, simply through an integration on the theoretical distribution of ΔI , namely

$$A_I = N_{CE} \int_{-\infty}^{+\infty} \Delta I f(\Delta I) d\Delta I. \quad (30)$$

However, one should pay attention to the symmetry of $f(\Delta I)$ between the positive and negative branches due to the even distribution of θ_0 and $\tilde{\lambda}_T$, whereby the above integration will always be 0.

Nevertheless, as discussed in the previous section, the magnitude of A_I actually goes up as N_{CE} increases. Inspired by that, in this section we try to estimate A_I through random walk method.

Concretely, let us define

$$M_I \equiv N_{CE} s_I^2. \quad (31)$$

Acceptable approximations bring that $\bar{\Delta I} \approx 0$ and $N_{CE}/(N_{CE} - 1) \approx 1$, which makes

$$M_I \approx \sum_{i=1}^{N_{CE}} \Delta I_i^2. \quad (32)$$

M_I indicates the variance of the distribution of ΔI and is integrable, namely

$$M_I = N_{CE} \int_{-\Delta I_\mu}^{\Delta I_\mu} \Delta I^2 f(\Delta I) d\Delta I, \quad (33)$$

where ΔI_μ is the ceiling on ΔI in realistic cases.

In practice, due to the difficulty of solving the analytic expression for $f(\Delta I)$, we numerically generate a large sample of ΔI based on the respective distributions of pertinent variables, whereupon M_I can be obtained by Eq. (31).

Now Eq. (11) can be alternatively written as

$$E(|A_I|) = \sqrt{\frac{2}{\pi} M_I}, \quad (34)$$

and surely, $E(|G_I|) = 2E(|A_I|)$. The above formulas are applicable to eccentricity as well.

2.4. The relation between the cumulative effect and the mass of Plutino

Now we verify the above theories on the number of CEs and cumulative effect. First, we modify the mass of Plutino ranging from 10^{-3} to 10^3 Pluto mass, while keep the orbital elements of Plutino and Trojan constant, to see if the theoretical predictions on N_{CE} , $A_I(A_e)$, $G_I(G_e)$ and $M_I(M_e)$ are consistent with the numerical simulations.

Fig. 5 shows the result of a number of simulations, generally lasting for 1Gyr, but terminated immediately if Trojan escapes from the resonant region. The consistency between the theory and simulations is satisfied fairly well, as least before the “knee”, where the duration of Trojan trapped in resonance drops significantly due to the increase of mass of Plutino. We can actually rectify the N_{CE} beyond the “knee” to the case that the simulation time instead lasts until 1Gyr, based on the uniform distribution of CEs with time. Concretely,

$$N_{CE} = N_{CE,res} \frac{t_{tot}}{t_{res}}. \quad (35)$$

The cyan points in (N) denote the rectified N_{CE} , which are consistent with the extended line of the theoretical predictions.

Recall the approximate distribution of ΔI in Paper I,

$$f(\gamma_I) = \frac{|\gamma_I|}{(1 + \gamma_I^2)^2}, \quad (36)$$

by which we can actually solve the correlation between v_P and M_I analytically.

Note that the derivations of Eq. (36) ignore the contributions of distributions of angular variables other than the CE distance R , but we can infer that these angular variables are

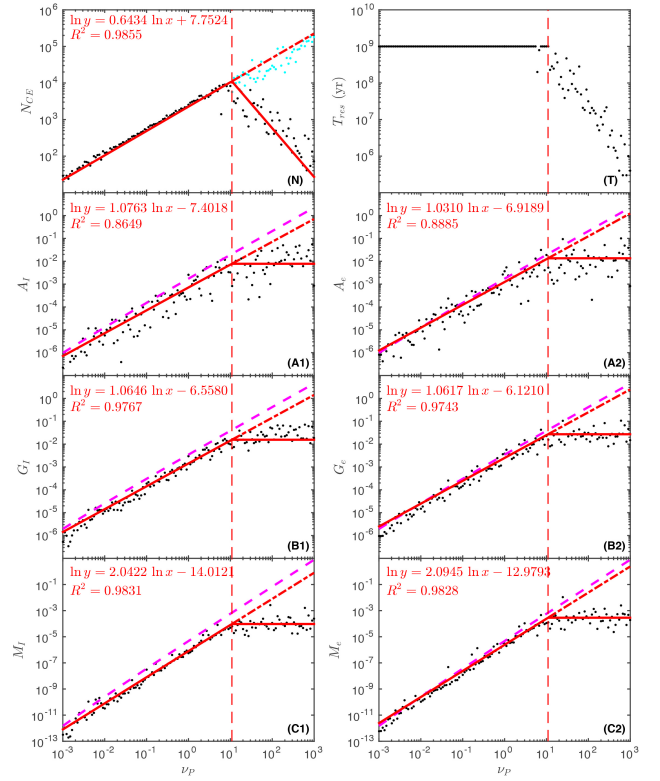


Figure 5. (N): N_{CE} . (T): t_{res} , the time that Trojan trapped in resonance. (A1) [(A2)], (B1) [(B2)], (C1) [(C2)] corresponds to $A_I(A_e)$, $G_I(G_e)$, $M_{2,I}(M_{2,e})$ respectively in a logarithmic scale. x -axis corresponds to the mass of Plutino v_P . Angular variables are in radian. Each dot represents the result from a numerical simulation including Plutino 1999CE119 and Trojan 2004UP10 with identical input parameters except the mass of Plutino. All simulations end with the escape of Trojan from the resonance region. The solid lines denote the theoretical predictions based on Sect. 2.3. The dashed lines in magenta denotes the predictions on the approximation formula based on Eq. (45). The knee in each plot(indicated by dashed vertical line) corresponds to the mass beyond which the evolution time drops significantly due to the untimely escape of Trojan. The specific value of the knee, along with the theoretical behaviors of the statistics after the knee, are predicted by a theory discussed later in Sect. 3. The cyan points on (N) denotes the expected number of CEs if Trojan stays in resonance till the end of simulation (1Gyr), based on Eq. (35). The results of power law fittings on the data before the knee are annotated on left top.

less related to the mass of Plutino. Concretely, combining (36) and (33), we have

$$M_I = N_{CE} \Delta I_0^2 \int_{-\gamma_{I_\mu}}^{\gamma_{I_\mu}} \gamma_I^2 \frac{|\gamma_I|}{(1 + \gamma_I^2)^2} d\gamma_I, \quad (37)$$

where $\gamma_{I_\mu} = \Delta I_\mu / \Delta I_0$ and

$$\Delta I_0 = \frac{m_P a_T}{m_S R_{th}} \sqrt{\frac{2(1 - e_T)}{1 + e_T}} \frac{1}{\sqrt{A - B \cos \max(I_P, I_T)}}. \quad (38)$$

We have roughly set $\sin \theta_0 = 1$, $\cos \lambda_T = 1$, and $\alpha_v = \max(I_P, I_T)$ here. The above integration gives

$$M_I = \chi_M v_P^2 (-1 + \varepsilon^2 - 2 \ln \varepsilon), \quad (39)$$

where

$$\chi_M = \left(\frac{a_T}{R_u} \right)^2 \left(\frac{2}{A - B \cos \max(I_P, I_T)} \right) \left(\frac{1 - e_T}{1 + e_T} \right) v_{Pluto}^2, \quad (40)$$

and

$$\gamma_{I\mu} = \pm \sqrt{\frac{1}{\varepsilon^2} - 1}. \quad (41)$$

Here ε actually represents the minimum scaled encountering distance, namely $\varepsilon \equiv R_\varepsilon / R_{th}$.

According to Eq. (17), if the minimum encountering distance is the radius within which the CE occurs at least once, we have

$$\varepsilon^2 \equiv \left(\frac{R_\varepsilon}{R_{th}} \right)^2 = \frac{1}{N_{CE}}. \quad (42)$$

Therefore,

$$R_\varepsilon = R_u, \quad (43)$$

Now make a 1st-order approximation of Eq. (39) and substitute ε with $1/\sqrt{N_{CE}}$, we have

$$M_I = \chi_M v_P^2 (-1 + \ln N_{CE}), \quad (44)$$

or alternatively

$$M_I = \chi_M v_P^2 \left(-1 + \ln \chi_N + \frac{2}{3} \ln v_P \right). \quad (45)$$

The logarithmic term here actually contributes little to the correlation between M_I and v_P . A peek at Fig. 6 gives $M_I \propto v_P^{2.1}$ approximately, which is in keeping with the fitting parameters of M_I annotated on Fig. 5.

Note that in Paper I, the final formulas for ΔI and Δe are quite similar other than the trigonometric terms associated with angular variables. Therefore, if we simply leave out these less significant terms, Eq. (45) is applicable to eccentricity as well.

In Fig. 5, we show the results of Eq. (45) for M_I (M_e), as well as the associated A_I (A_e) and G_I (G_e), in magenta dashed lines, which overestimate the effect a little, probably due to the coarse approximations of the angular terms in ΔI_0 and Δe_0 . Note that the results deviate more on inclination than eccentricity, which is conceivable since the approximation $\sin \theta_0 = 1$ is more unrealistic than $\cos \theta_0 = 1$ in view of the actual distribution of θ_0 ⁴. Notwithstanding, Eq. (45) can still be considered as a swift and convenient analytical formula to estimate the CE effect in practice.

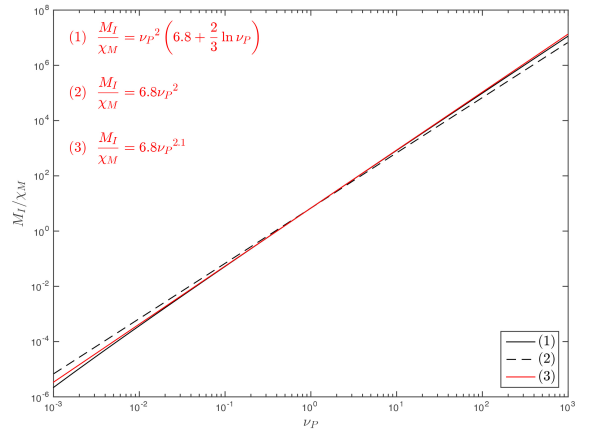


Figure 6. The comparison between Eq. (45) and two kinds of power law correlations. Note that $\ln \chi_N \approx 7.72$ for 1999CE119&2004UP10.

2.5. The aggregate effect of several (multiple) Plutinos

Suppose we now have \widetilde{N}_P Plutinos and the total mass is \widetilde{v}_P . The probability distribution function of mass $f(v_P)$ satisfies

$$\int_0^1 f(v_P) dv_P = 1, \quad (46)$$

and

$$\widetilde{N}_P \int_0^1 v_P f(v_P) dv_P = \widetilde{v}_P. \quad (47)$$

In view of Eq. (32), namely the approximate expression for M_I , the total contribution from all Plutinos is

$$\widetilde{M}_I = \sum_{k=1}^{N_P} \sum_{i=1}^{N_{CE}^{(k)}} (\Delta I_i^{(k)})^2, \quad (48)$$

whereupon expectation of the total effect is

$$|\widetilde{A}_I| = \sqrt{\frac{2}{\pi} \widetilde{M}_I} = \sqrt{\frac{2}{\pi} \sum_{k=1}^{N_P} M_I^{(k)}}, \quad (49)$$

which is equivalent to in a continuous case

$$|\widetilde{A}_I| = \sqrt{\frac{2}{\pi} \widetilde{N}_P \int_0^1 M_I(v_P) f(v_P) dv_P}, \quad (50)$$

where we assume that all the Plutinos have same orbital characteristics thus M_I merely concerns the specific mass of each Plutino.

Now we consider the mono-concentrated case, that only one Plutino possesses all the mass, namely $\widetilde{N}_P = 1$, $f(v_P) = \delta(v_P - \widetilde{v}_P)$, thus we have the corresponding total effect

$$|\widetilde{A}_{I,0}| = \sqrt{\frac{2}{\pi} M_I(\widetilde{v}_P)}. \quad (51)$$

⁴ Refer to Paper I for the concrete expression for ΔI and Δe

The evenly-distributed case implies the other extreme, that the total mass is evenly distributed among all the Plutinos, namely $f(\nu_P) = \delta(\nu_P - \tilde{\nu}_P/\tilde{N}_P)$, thus we have

$$|\widetilde{A_{I,*}}| = \sqrt{\frac{2}{\pi} \widetilde{N}_P M_I \left(\frac{\tilde{\nu}_P}{\widetilde{N}_P} \right)}. \quad (52)$$

Now we prove that for arbitrary mass distribution function $f(\nu_P)$, it always stands up that

$$|\widetilde{A_{I,*}}| \leq |\widetilde{A}_I| \leq |\widetilde{A}_{I,0}|. \quad (53)$$

Given Eq. (47), the above inequality is equivalent to

$$M \left[\int_0^1 x f(x) dx \right] \leq \int_0^1 M(x) f(x) dx \leq \frac{M(\bar{x})}{\bar{x}} \int_0^1 x f(x) dx, \quad (54)$$

where $x \equiv \nu_P$, $\bar{x} \equiv \tilde{\nu}_P$, and the subscript is omitted for simplicity. By the first mean value theorem for definite integrals, it is easy to prove the right inequality sign, as long as $H'(x) > 0$, where $H(x) = M(x)/x$. For Eq. (45), the above requirement is always satisfied in consideration of the natural constraint $M_I \geq 0$. Meanwhile, the left one is actually a special form of Jensen's inequality, since $M''(x) > 0$ indicates $M(x)$ is a convex function.

Inequation (53) interprets that the more concentrated the mass is, the larger the total effect will be. The maximum effect occurs when all the mass concentrates on one single Plutino, while the minimum effect occurs when the mass evenly distributes among all the Plutinos.

Now if we roughly propose that $M_I \propto \nu_P^2$, Eq. (52) leads to

$$|\widetilde{A_{I,*}}| \propto \frac{1}{\sqrt{\widetilde{N}_P}}, \quad (55)$$

which means the total effect deceases with a power law as the number of Plutinos increases when all the Plutinos have the same mass.

Consequently we can give a coarse estimation of the upper limit of the aggregate CE effect in reality. Basically we can assert that the total mass of Plutinos in reality is less than 10 times Pluto mass. Assuming all the Plutinos have the same orbital characteristics as 1999CE119, the approximate formula gives $|\widetilde{A}_{I,0}| \approx 1^\circ$ in the mono-concentrated case. However, this is obviously unrealistic since the Pluto is already the largest Plutino, under which condition, the best situation will be 10 Plutinos with Pluto mass each. Thereupon the total effect decreases to $1^\circ / \sqrt{10} \approx 0.3^\circ$, which is a quite small perturbation and barely makes any significance. We should notice that this result is already a higher expectation of the upper limit of total effect, in consideration of the overestimation of Eq. (45), as well as 1999CE119 is an example causing comparably large effect considering its small inclination and high eccentricity, which will be further discussed later.

The above analysis can be done in the same way for the effect on eccentricity as well. We leave out the concrete analysis here, considering that the magnitude of eccentricity

change is basically close to that of inclination, whereupon CEs between Plutino and Trojan barely influence the eccentricity of Trojan either.

2.6. The relation between the cumulative effect and the inclination of Plutino

Now we verify if our theory works when the inclination of Plutino changes. We use two pairs 1999CE119&2004UP10 and 2001FU172&2004UP10 as templates, while artificially varying the initial inclination of Plutino from 0° to 30° in the numerical simulation, to seek out the influence of I_P on the CE times and cumulative effect. Fig. 7 shows the variations of N_{CE} , A_I and A_e as I_P increases both numerically and theoretically. Note that the input orbital elements passed to the theoretical algorithm are mean values in the numerical simulations.

We can notice that N_{CE} , A_I , A_e all come down as I_P increases, but in a relatively small range, compared to the effect of mass in Fig. 5. The peak appears when the inclination of Plutino is close to that of Trojan, clearest in (N), which agrees with the intuition. The theoretical predictions basically match the numerical results, while the cusps may result from the random deviation when numerically implementing the algorithm.

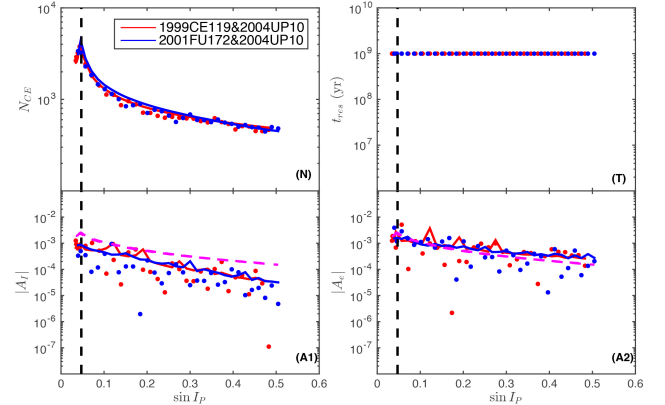


Figure 7. (N): N_{CE} . (T): t_{res} , the time that Trojan trapped in resonance. (A1), (A2): A_I , A_e versus $\sin I_P$. A_I are in radian. Each dot represents a numerical simulation with identical input parameters except the initial inclination of Plutino (Red for 1999CE119 and blue for 2001FU172). The Trojan is fixed to 2004UP10. The solid curves denote the theoretical predictions based on Sect. 2.3. The dashed curves in magenta denote the results based on Eq. (34) and (45). The dashed line indicates the mean inclination of Trojan.

2.7. The relation between the cumulative effect and the inclination of Trojan

For sure, the inclination of Trojan will affect CE as well. Intuitively, the more inclined, the less chance will Trojan encounters Plutino, which agrees with the simulation results in Fig. 8. As expected, the number of CEs and cumulative effect reach the peak when the inclination of Trojan is close

to that of Plutino. The theoretical predictions are basically consistent with the simulation results.

Furthermore, back to our starting point on the high inclination problem of Trojan, we seem to find a possible explanation here, that Trojans with low inclinations will interact with Plutinos more strongly, whereupon increasing their inclinations, thus bringing about the deficiency of Trojans with low inclination in reality. However, as previously discussed, the total CE effect on inclination will be less than 1° even for a extreme case where the overall mass of Plutinos is up to 10 Pluto mass and at the same time all Trojans and Plutinos posses low inclinations. Hence there is barely any room for the inclination of Trojan to play a selective role. Despite the fact, this mechanism may work for other planet systems under certain conditions.

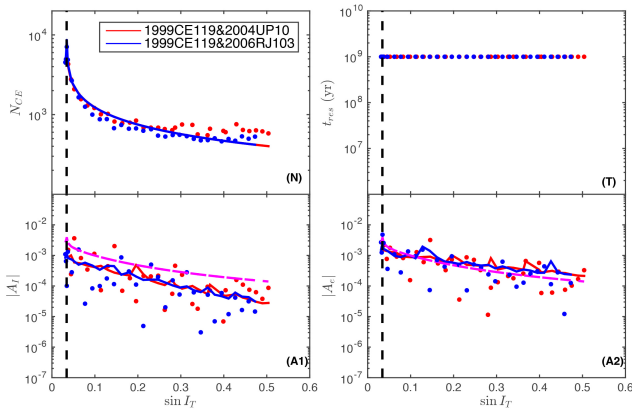


Figure 8. Similar to Fig. 7 but versus I_T and only initial I_T in the simulation varies. The dashed line indicates the mean inclination of Plutino.

2.8. The relation between the cumulative effect and the eccentricity of Plutino

Generally, actual Trojans are in near circular orbits, whereupon we leave out the discussion on the eccentricity of Trojan here. Yet, the eccentricity of Plutino matters, directly determining whether or not CE will happen. Fig. 9 shows the behaviors of N_{CE} , A_l and A_e as e_P varies, including numerical simulations and theoretical evaluations. We perceive that the CE effect rises first then drops off as e_P increases, reaching the peak within the yellow region. As expressly defined in the caption, the yellow region represents the range of eccentricity where the perihelion of Plutino lies between the perihelion and aphelion of Trojan, in which case the interaction naturally becomes strongest. Note that when the perihelion of Plutino is larger than the aphelion of Trojan, the orbits should not intersect geometrically, yet the simulations still produce a number of CEs, which is due to the fluctuation of orbital elements during the evolution.

The theoretical predictions basically reflect the overall trend, whereas behave poorly at a very low eccentricity. This is because when the eccentricity of Plutino is considerably

low, Eq. (20) fails to produce a solution, whereupon to avoid a remarkable truncation, we roughly set the width of the encounter region W to be the perimeter of the orbit of Trojan, which is supposed to be infinite. This manipulation gives rise the abnormal number of CEs when the orbits are separated far away from each other.

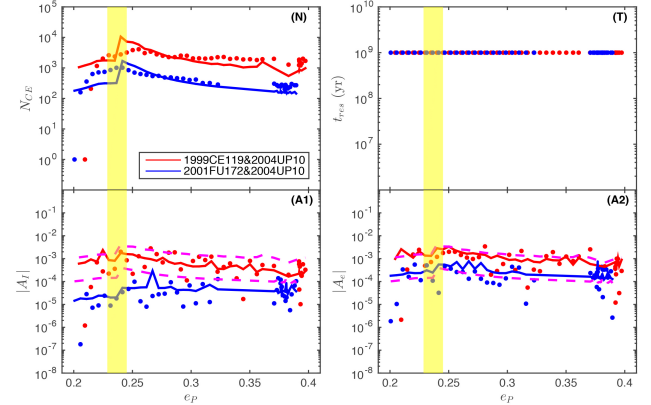


Figure 9. Similar to Fig. 7 but versus e_P and only initial e_P in the simulation varies. The highlight region is confined by e_E and e_X where $a_T(1 - e_T) = a_P(1 - e_X)$ and $a_T(1 + e_T) = a_P(1 - e_E)$. Some dots are missed because there is none CE, which can not be displayed in a logarithmic plot.

Rather interesting is that in Fig. 9 Plutinos with high inclinations (2001FU172) tend to evolve into orbits with large eccentricities, which is not that evident for Plutinos with low inclinations (1999CE119). This phenomenon is more clearly revealed in Fig. 10, where the initial and mean orbital elements of Plutinos in simulations are shown simultaneously. Since our model merely includes one giant planet Neptune, it may originate in the unstable interactions with Neptune when Plutino takes some specific value of eccentricity, which is believed to be discussed by predecessors already. [reference quest](#)

2.9. The relation between the cumulative effect and the libration amplitude

In Almeida et al. the libration amplitude of Plutino or Trojan is believed to have a significant effect on the close encounter, and the larger the amplitude is, the higher the encounter chance will be. On the contrary, we propose that the libration amplitude barely contributes to CE, either in the number of times or the interaction effect. Seemingly is that a large libration amplitude will increase the area of orbital overlap, whereas one should notice that it is not the area but kinds of flux that determines the chance of CE. Figuratively, if we record the position of Plutino every 1 yr and project the coordinates onto a plane, the obtained points, which represent the occurrence frequency of Plutino within a given time, will become sparser at a larger libration amplitude, whereupon the chance of CE will not necessarily rise, despite the expansion of overlapping area.

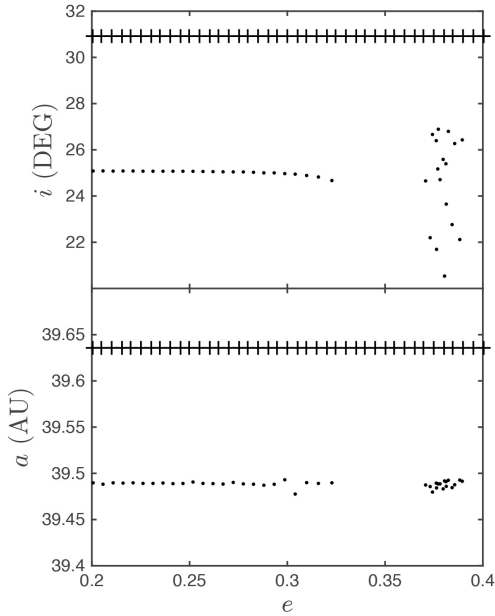


Figure 10. The initial and mean orbital elements of Plutino in numerical simulations we operated in Fig. 9, denoted by “+” and “-” respectively.

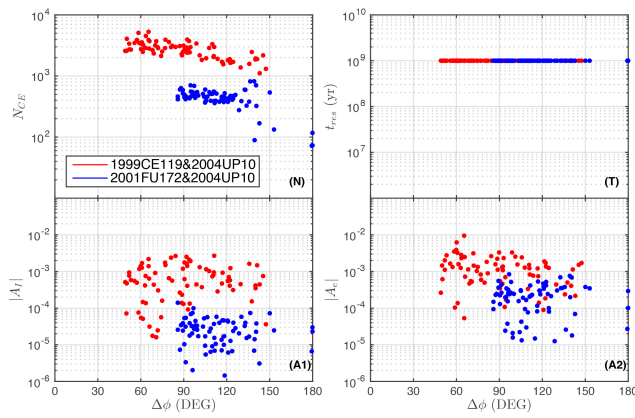


Figure 11. Similar to Fig. 7 but versus $\Delta\phi_p$. The initial Ω_p , ω_p and M_p for the simulations are randomly generated while other orbital elements are held. The libration amplitude plotted is the average value during the simulation. The dots with amplitude close to 180° may not factually represent stable libration orbits.

To test it, we randomly modify the initial value of Ω , ω and M of Plutino, *ceteris paribus*, in the numerical simulations, then pick out the stable orbits to count the CE times and CE effects, corresponding to the average libration amplitude during evolution. The same method can be applied for the effect of the libration amplitude of Trojan as well. The simulation results are shown in Fig. 11 and Fig. 12 respectively, where clearly the increase of libration amplitude of either Plutino or Trojan brings no prominent effect on the CE effect, even

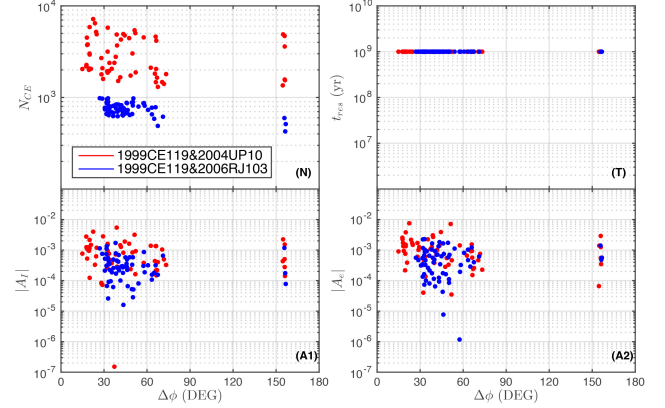


Figure 12. Similar to Fig. 7 but versus $\Delta\phi_T$. The initial Ω_T , ω_T and M_T for the simulations are randomly generated while other orbital elements are held. The libration amplitude plotted is the average value during the simulation. The two clusters may correspond to the “tadpole” and “horseshoe” orbits of Trojan respectively.

slightly decreasing the number of CEs, which accords with our expectations.

Note that our previous theoretical algorithm is free from the libration amplitude of Plutino and Trojan. Therefore the theoretical predictions are missed here.

2.10. The dependency of the theoretical algorithm on the artificial parameter κ_f

To sum up, our theoretical algorithm on CE effect take the following variables into account: v_P , a_P , e_P , I_P , Ω_T , ω_T , t_T , I_T . In previous sections we have paid great effort to check out the performance of the algorithm on these variables and the result is acceptable. Nevertheless, our algorithm contains an artificial parameter κ_f , as mentioned in Paper I, which is actually less influential.

Specifically, here we examine the impact of κ_f with several tests. For better understanding, we now use $\sigma_f \equiv 1/\sqrt{\kappa_f}$ to replace κ_f in the following examination. In Fig. 13 we modify σ_f from 0.1° to 5° to observe the variation of A_I (A_e) and s_I (s_e) for two planetesimal pairs. We can find that s_I (s_e), namely the key indicator of the distribution, barely varies as σ_f increases, in keeping with the simulated results fairly well for either planetesimal pair, albeit with some random deviation in the the numerical implementation of the algorithm. The top plots depict A_I (A_e), which basically remains constant as well, deviating a little bit from the simulated value, mainly resulting from the inaccuracy of the random walk theory, as shown in Fig. 3.

Consequently we believe that our theoretical algorithm is insensitive to the free parameter κ_f . In practice, one can either apply the empirical formula given above, or more roughly choose a fixed value of κ_f .

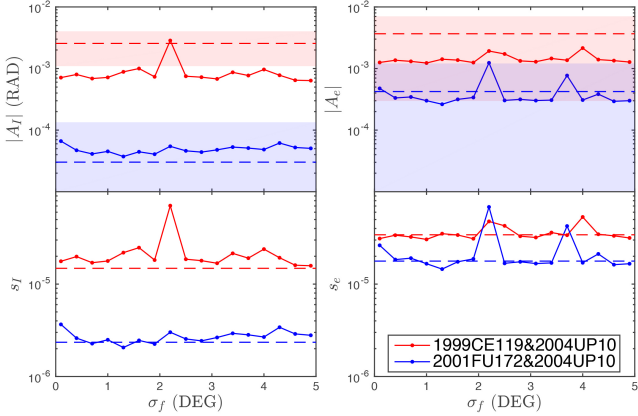


Figure 13. The performance of the theoretical algorithm on CE effect as the free parameter $\sigma_f \equiv 1/\sqrt{k_f}$ varies. The left and right columns correspond to the effects on the inclination and eccentricity of Trojan respectively. The top and bottom panels correspond to the cumulative effect $|A_I|$ ($|A_e|$) and the standard deviation s_I (s_e) of the distribution of CE effect defined by Eq. (10), respectively. On each plot, solid and dashed curves denote the result derived by the theoretical algorithm and numerical simulations respectively. The color strips indicate the 95% confidence interval of the numerical cumulative effect, i.e. the dashed curves.

3. THE MIXED STRATEGY AND MAXIMUM PERTURBATION APPROXIMATION

We have found that the communications between Plutinos and Trojans have barely any influence on the orbital elements of Trojans in reality. However, in Fig. 5, we perceive that a Plutino with sufficiently large mass is able to drive out Trojan from its resonance region within a limited time. If this kind of effect is achievable in reality and at the same time selective to the inclination of Trojan, it may thus indirectly change the distribution of the inclination of Trojan. Therefore in this section we will first explore the detailed mechanism behind the “knee” in Figure 5 and then apply it to the discussion of the aggregate effect under a cluster of Plutinos in reality.

3.1. Mass-dominating escape

First, we are interested in how close the Plutino approaches the Trojan will it exert a perturbation capable of influencing the stability of Trojan in 1:1 resonance. Since this perturbation acts prominently only within a relatively short time, the impulse will be an appropriate quantity to measure the effect.

Therefore, by integrating the perturbing acceleration exerted by Plutino from the entrance of the CE region to the exit, and under the simplification that the trajectory of Plutino is a straight line as mentioned above, we have the perturbing impulse

$$v_I = \int_{t_E}^{t_X} f_{ptb} dt = \int_{\theta_E}^{\theta_X} f_{ptb} \frac{d(b \tan \theta_E + b \tan \theta)}{V_{rlt}}, \quad (56)$$

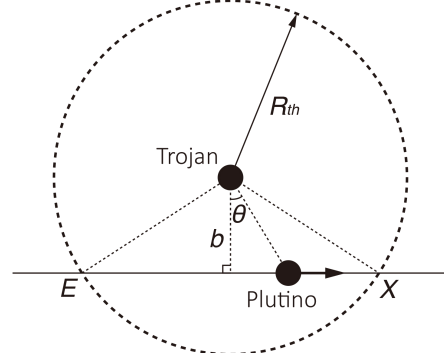


Figure 14. The illustration for Plutino flying past Trojan.

where b is the minimum distance in CE and

$$V_{rlt} = V_P - V_T = \sqrt{\mu_S \left(\frac{2}{a_T} - \frac{1}{a_P} \right)} - \sqrt{\frac{\mu_S}{a_T}}. \quad (57)$$

The perturbing acceleration is simply

$$f_{ptb} = \frac{\mu_P}{(b/\cos \theta)^2} \cos \theta, \quad (58)$$

where the horizontal component is left out due to the symmetry. Thereupon the final result for v_I gives

$$v_I = \frac{\mu_P}{b V_{rlt}} \int_{\theta_E}^{\theta_X} \cos \theta d\theta \approx \frac{\mu_P}{b V_{rlt}} \int_{-pi/2}^{pi/2} \cos \theta d\theta = \frac{2\mu_P}{b V_{rlt}}. \quad (59)$$

On the other hand, supposing that in a restricted 3-body model, the momentum required for the stability of Trojan is provided by the force of Neptune, we have in rough

$$v_M = \sqrt{\frac{2\mu_N}{a_T}}. \quad (60)$$

When the above two quantity is comparable, namely $v_I \approx v_M$, the Plutino is likely to influence the behavior of Trojan, whereupon the minimum distance in this case is

$$R_k = \chi_k v_P, \quad (61)$$

where

$$\chi_k \equiv 2^{1/2} v_{Pluto} v_{Nep}^{-1/2} \left[\sqrt{\frac{1}{a_T} \left(\frac{2}{a_T} - \frac{1}{a_P} \right)} - \frac{1}{a_T} \right]^{-1}, \quad (62)$$

and

$$v_{Nep} \equiv \frac{m_{Neptune}}{m_S}. \quad (63)$$

We can name R_k the kinetic radius in CE, compared with R_u , proposed in Eq. (28), might as well named the kinematic radius in CE. To sum up, R_k , basically proportional to the mass of Plutino, is strictly connected with the interactions between Plutino and Trojan within the CE region, while R_u , oppositely irrelevant to the mass of Plutino, is manipulated

by the orbital movements of Plutino and Trojan around the Sun, in which case the mass of Plutino becomes trivial.

Now by combining the above two encountering radii together, a fine explanation to the turning point (knee) in Fig. 5 can be put forward, which is visually shown in Fig. 15. The upper plot here is directly copied from (N) in Fig. 5 for comparison. In the lower plot, each dot corresponds to the minimum encountering radius R_e reached in the simulation in Fig. 5. R_e first remains basically unchanged as ν_P increases, then dramatically goes up when ν_P becomes greater than a particular value, forming a knee located at basically the same value of ν_P as Fig. 5 shows.

Interestingly, in Fig. 15 the knee appears exactly at the intersection of R_k and R_u , indicating that the minimum encountering radius R_e should actually be greater than the larger one between the two. An explicit picture gives that when the possible encountering radius R_u is lower than the kinetically allowable radius R_k , chance emerges that the Plutino approaches closely enough to exert perturbing impulse comparable to the constraining momentum of Trojan contributed by Neptune, thus likely to expel the Trojan from the resonant region. Besides, as ν_P and R_k continue to rise, the chance becomes even larger, thus leading to the drop of N_{CE} and reduction of resonant time of Trojan.

In the case that the mass of Plutino is greater than the threshold mass $\nu_{P,th} \approx 10.9$, similar to Eq. (42), we can assume that once occurs a CE with encountering radius less than R_k , the Trojan will be expelled. Thereupon the total number of CEs satisfies

$$\frac{1}{N_{CE}} = \left(\frac{R_k}{R_{th}} \right)^2. \quad (64)$$

Hence,

$$N_{CE} (\nu_P > \nu_{P,th}) = \chi_N^* \nu_P^{-4/3}, \quad (65)$$

where

$$\chi_N^* \equiv \frac{\kappa_{th}^2}{2 \cdot 3^{2/3}} \left[\sqrt{\frac{a_P}{a_T} \left(\frac{2a_P}{a_T} - 1 \right)} - \frac{a_P}{a_T} \right]^2 \nu_{NeP} \nu_{Pluto}^{-4/3} \quad (66)$$

The descending branch in the upper plot in Fig. 15 basically conforms to the above equation. Therefore the theoretical estimations on the parts beyond “knee” of cumulative effect in Fig. 5 can be implemented simply, based on the already derived $N_{CE} (\nu_P > \nu_{P,th})$.

One may notice that in the lower plot in Fig. 15, the data point deviates a little from R_k when ν_P is relatively high, which is probably due to the straight line approximation of the trajectory of Plutino in CE, giving rise to a higher estimation of the perturbing impulse, than a hyperbola trajectory in real cases. But anyhow, we seldom run into a planetesimal with this large mass in reality.

We have figured out the mechanism behind the escape of Trojan when the mass of Plutino is sufficiently large. However, in reality, it is impossible that there exists a Plutino with mass up to 10 times Pluto mass, due to which, even for a

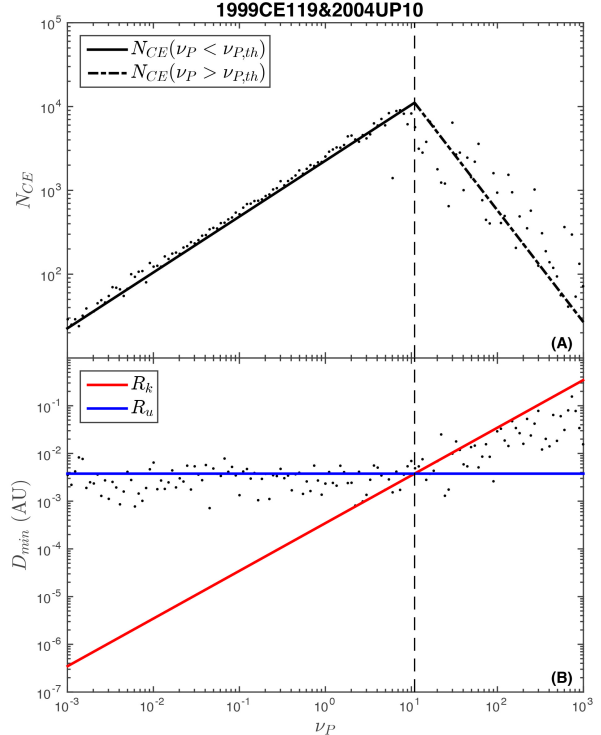


Figure 15. (A): N_{CE} versus mass of Plutino, same as (N) in Fig. 5. Solid curves are theoretical results for $\nu_P < \nu_{P,th}$ and $\nu_P > \nu_{P,th}$ respectively. (B): The minimum encountering radius R_e reached in each simulation in Fig. 5 with respect to the mass of Plutino. The solid curves denote the kinetically minimum encountering radius R_k and the kinematically minimum encountering radius R_u respectively, which are derived theoretically. The dashed line indicates the position of the intersection of the two radii, namely the threshold mass $\nu_{P,th}$.

Plutino with remarkably low inclination and relatively large eccentricity like our example 1999CE119, this mechanism is hard to be triggered.

3.2. Mixed strategy and times-dominating escape

Although the Plutino in reality is unlikely to expel Trojan with enough mass, it may manage it by sufficient number of CEs alternatively, for the minimum encountering radius can be arbitrarily small so long as there are enough CEs.

Fig. 16 shows the relationship between the minimum encountering radius and the number of CEs for the case including Plutino 1999CE119 with Pluto mass and Trojan 2004UP10. The data derived from the numerical simulations including one Plutino (the filled circle) or several cloned Plutinos (crosses)⁵ basically obey a negative correlation, situated closely along the theoretical result for R_e based on Eq. (42).

⁵ The clone method is same as above.

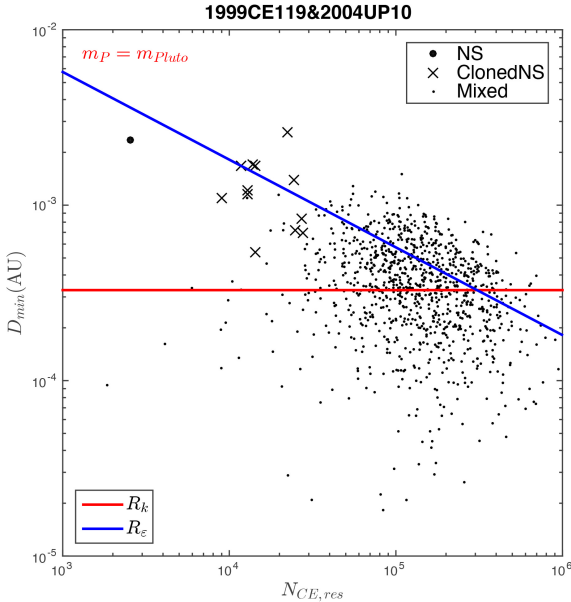


Figure 16. The minimum encountering radius with respect to CE times. The filled circle is derived from the numerical simulation for 2004UP10 and 1999CE119 with Pluto mass. The crosses are derived from the numerical simulation for 2004UP10 and several clones for 1999CE119, each with Pluto mass. The dots are derived from mixed simulations with 2004UP10 and simulated perturbations from 1999CE119 with Pluto mass, including 10^6 CEs. The red and blue lines are the theoretical results for R_k and R_ε respectively.

Here we will introduce a new method to break the natural limitation of number of CEs in the numerical simulation, and simultaneously retain the dynamic evolution. Simply and directly, here comes the idea that we can combine the numerical simulation and the M-C method mentioned in Paper I into a mixed strategy. Specifically, we numerically simulate a 3-body model including the Sun, the Neptune and the test particle Trojan, during which we simulate the perturbation of Plutino using the M-C method at some randomly picked out steps, then alter the orbital elements of Trojan in the numerical simulation according to the randomly simulated perturbing effect, and keep going until the escape of Trojan from the resonant region. This mixed strategy is able to generate as many CE times as required by merely increasing the portion of steps where the simulated CE is inserted, and at the same time show the overall perturbing effect such as the escape of Trojan in the numerical simulation.

Fig. 16 contains the results derived from 1000 sets of mixed simulations, which is denoted by a cloud of small dots. All the simulations have identical input parameters, such as the mass of Plutino, fixed to Pluto mass, and the CE ratio, namely the portion of steps into which simulated CE is inserted among the total steps. We see that the dots roughly distribute along the minimum encountering radius

line $R_\varepsilon = R_\varepsilon(N_{CE})$, and blocked by R_k , beyond which the Trojan will be expelled as previously discussed. Note that although we have forced more than 10^6 CEs into the numerical simulations, few cases live through all the CEs, most of which stop before the intersection between R_ε and R_k , which evidently proves that enough CEs can also lead to the escape of Trojan, despite of a Plutino with low mass. In addition, this consistency likewise verifies the theoretical analysis on the balance between R_k and R_ε discussed above.

3.3. The aggregate effect of several Plutinos

However, only one Plutino is impossible to produce such a large number of CEs in reality in order to expel Trojan, as denoted by the filled circle in Fig. 16. Therefore we need to focus on the aggregate effect of a cluster of Plutinos. The question goes that whether the CE effect will be heightened as more and more Plutinos share a fixed total mass, in other words, whether the reduction of minimum encountering radius R_ε due to the increase in the number of CEs brought by more Plutinos, will catch up with the reduction of the kinetic radius R_k due to the decrease of the mass of each Plutino. To figure out this, we will theoretically explore R_ε and R_k in the case including multiple Plutinos below.

Now suppose the total mass of Plutinos is $\tilde{m}_P = 10 m_{Pluto}$, which is a quite large assumption, and the total number of Plutinos is N_P . Assuming that all the Plutinos is identical with 1999CE119, and own same mass, thus the total number of CEs is

$$\widetilde{N}_{CE} = N_P N_{CE}, \quad (67)$$

while according to Eq. (25), the number of CEs contributed by each Plutino is

$$N_{CE} = \chi_N \left(\frac{\tilde{v}_P}{N_P} \right)^{2/3}, \quad (68)$$

where $\tilde{v}_P \equiv \tilde{m}_P / m_{Pluto}$.

Thereupon, with Eq. (42) immediately we have

$$R_\varepsilon = \frac{R_u}{\sqrt{N_P}}. \quad (69)$$

On the other hand, the kinetic radius R_k shrinks for the decease of mass of Plutino, namely

$$R_k = \chi_k \frac{\tilde{v}_P}{N_P}. \quad (70)$$

Obvious is that R_k decreases faster than R_ε , which is visually shown in Fig. 17. We see that when $N_p = 1$, namely only one Plutino with 10 times Pluto mass, which is close to the mass threshold in Fig. 15, R_ε approaches R_k , whereas as there are more Plutinos sharing the mass, R_k becomes way smaller than R_ε , making the escape of Trojan almost impossible. Note that in reality the mass of Plutino should not be larger than Pluto mass, thus in this case necessarily $N_P \geq 10$, which is denoted by the dashed line in Fig. 17.

To wrap up, the division of mass will result in the reduction of the probability of Trojan escaping the resonant region,

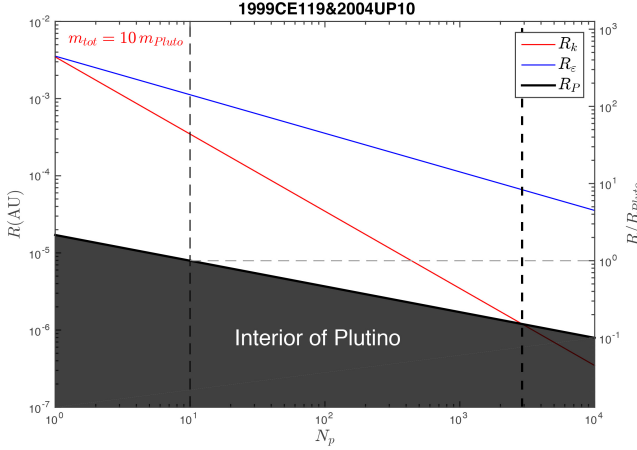


Figure 17. The variation of R_e , R_k and R_P as more Plutinos share the total mass. The dashed line denotes $N_p = 10$, where the mass of each Plutino equals Pluto mass, namely the upper limit in reality. The thick dashed line denotes where $R_P = R_{P,c}$, beyond which the definition of R_k is invalid and Plutinos become unable to expel Trojan from its resonance merely by close encounters.

which is similar to the conclusion in Sect. 2.5. Since we have focused on the case with total mass exaggerated, and Plutino (1999CE119) exerting relatively large CE effect, it will be even more difficult for Plutinos in reality to expel Trojan from its resonant region.

Note that in Fig. 17, as the mass of each Plutino shrinks, R_k will finally cross R_P , which is the physical radius of Plutino, simply estimated by the characteristics of Pluto, namely

$$R_P = R_{Pluto} \left(\frac{\tilde{v}_P}{N_p} \right)^{1/3}, \quad (71)$$

where R_{Pluto} is the physical radius of Pluto. When $R_k < R_P$, clearly the mechanism introduced in Sect. 3.1 is forbidden, thus the definition of R_k becomes invalid. Simple derivations give that

$$\frac{R_P^c}{R_{Pluto}} = \left(\frac{R_{Pluto}}{\chi_k} \right)^{1/2} \approx 0.15. \quad (72)$$

That is, merely by close encounters, a Plutino with radius smaller than the critical value R_P^c is unable to influence the resonance of Trojan significantly. In other words, a such small Plutino may take collisions as a major way to exert its influence.

One may find that in Fig. 17, if N_p is considerably large, R_e will cross R_P as well. Similarly, we have the critical value

$$\frac{R_P^d}{R_{Pluto}} = \tilde{v}_P \left(\frac{R_{Pluto}}{R_u} \right)^2. \quad (73)$$

Within 1 Gyr, given the total mass of Plutinos $\tilde{v}_P = 10$, $R_P^d/R_{Pluto} \approx 5 \times 10^{-5}$ or $R_P^d \approx 50$ m. That is, a swarm of identical Plutinos will reach a minimum encountering radius close to their own physical radius, if their radius is smaller than R_P^d . In other words, collisions with Trojan will become

frequent for a swarm of such small Plutinos with given total mass.

In summary, for a swarm of identical Plutinos with a fixed total mass, if the radius of each Plutino $R_P \gtrsim R_P^c$, the expelling influence of close encounters is possible, while if $R_P \lesssim R_P^d$, the effect of collisions becomes dominant. As for the Plutinos with radius in between, it seems that neither effect is effective. Of course the reality is way more complicated, but by grouping sizable planetesimals, the above analysis can be applied qualitatively as well.

3.4. Mass distribution function and CE intensity factor

Similar to Sect. 2.4, for practical convenience, here we further discuss the relation between R_e and R_k given a specific mass distribution function of Plutinos.

First of all, the mass distribution function $f(v_P)$ should satisfy Eq. (46) and (47). Now given the total mass \tilde{v}_P and total number of Plutinos \tilde{N}_P , we have the number of Plutinos with mass v_P locating within $(v_P, v_P + dv_P)$

$$dN_P = \tilde{N}_P f(v_P) dv_P \quad (74)$$

According to Eq. (25), the number of CEs contributed by this mass section of Plutinos is

$$dN_{CE} = N_{CE}(v_P) dN_P \quad (75)$$

And by Eq. (69) the minimum encountering radius R_e reached by this section of Plutinos is

$$R_e(v_P) = \frac{R_u}{\sqrt{dN_P}}, \quad (76)$$

which is similar to Eq. (69).

We must realize that R_k and R_e can not be directly compared since they are both the function of mass v_P . Therefore to explore the total effect we need to normalize the contribution by each mass section to a standard mass, where the number of CEs can be added up to solve R_e , which can be compared with the corresponding R_k .

Consequently, we introduce the CE intensity factor defined as

$$\tau(v_P) \equiv \frac{R_k(v_P)}{R_e(v_P)} \quad (77)$$

A simple idea comes that if $R_k > R_e$ at a specific mass, namely Trojan fails to escape with regard to the contribution by this mass section, the relation should also be satisfied when the contribution is normalized to a standard mass. In other words, $\tau(v_P)$ should remain constant when the reference mass varies. Now we might as well take the Pluto mass as the standard mass, whereupon

$$\tau_1(v_P) = \tau(v_P). \quad (78)$$

The normalized minimum encountering radius can thus be obtained as

$$R_{e,1}(v_P) = \frac{R_k(v_P = 1)}{\tau(v_P)} = \frac{R_u}{v_P \sqrt{dN_P}}. \quad (79)$$

This is equivalent to the effect reached by $N_{CE,1}(\nu_P)$ CEs at the standard mass, where

$$N_{CE,1}(\nu_P) = \left[\frac{R_{th}(\nu_P = 1)}{R_{\varepsilon,1}(\nu_P)} \right]^2 = \left(\frac{R_{th,1}}{R_u} \right)^2 \nu_P^2 dN_P \quad (80)$$

and $R_{th,1} \equiv R_{th}(\nu_P = 1)$. We can now add up the number of CEs contributed by all mass sections at this reference mass, namely

$$\widetilde{N_{CE,1}} = \left(\frac{R_{th,1}}{R_u} \right)^2 \int_0^1 \nu_P^2 dN_P. \quad (81)$$

Therefore the minimum encountering radius reached by all mass sections is

$$\widetilde{R_{\varepsilon,1}} = \frac{R_{th,1}}{\sqrt{\widetilde{N_{CE,1}}}} = \frac{R_u}{\sqrt{\int_0^1 \nu_P^2 dN_P}} = \frac{R_u}{\sqrt{\widetilde{N}_P \int_0^1 \nu_P^2 f(\nu_P) d\nu_P}}. \quad (82)$$

The aggregated intensity factor is

$$\widetilde{\tau}_1 = \frac{R_{k,1}}{\widetilde{R}_{\varepsilon,1}}. \quad (83)$$

Since the intensity factor is independent of the reference mass, we have

$$\widetilde{\tau} = \widetilde{\tau}_1 = \frac{\chi_k}{R_u} \sqrt{\widetilde{N}_P \int_0^1 \nu_P^2 f(\nu_P) d\nu_P} \quad (84)$$

We now consider some extreme cases to verify the above formula. For a evenly distributed case, the mass of each Plutino is identically $\nu_P^* = \widetilde{\nu}_P / \widetilde{N}_P$, whereupon the mass distribution function is

$$f(\nu_P) = \delta(\nu_P - \nu_P^*) \quad (85)$$

According to Eq. (82), the minimum encountering radius reached by all these Plutinos is

$$\widetilde{R}_{\varepsilon,1} = \frac{R_u}{\nu_P^* \sqrt{\widetilde{N}_P}}. \quad (86)$$

And the aggregated intensity factor based on Eq. (84) is

$$\widetilde{\tau}_* = \frac{\chi_k \widetilde{\nu}_P}{R_u} \frac{1}{\sqrt{\widetilde{N}_P}} \quad (87)$$

We can clearly find that as N_P rises, CE intensity decreases. Now if we normalize $\widetilde{R}_{\varepsilon,1}$ back to the case where the reference mass equals ν_P^* , the minimum encountering radius will be the same as Eq. (69), which is precisely the result from the discussion on a evenly distributed case in a direct way, namely

$$\widetilde{R}_\delta = \widetilde{R}_{\varepsilon,1} \nu_P^* = \frac{R_u}{\sqrt{\widetilde{N}_P}}. \quad (88)$$

Specifically, when $\widetilde{N}_P = 1$, we have $\widetilde{\nu}_P = \nu_P^*$, $R_\varepsilon = R_u$, $R_k = \chi_k \widetilde{\nu}_P$, which we may call the mono-concentrated case.

Naturally, in this case the CE effect will reach the highest, where the intensity factor will be

$$\widetilde{\tau}_m = \frac{\chi_k \widetilde{\nu}_P}{R_u}. \quad (89)$$

By set $M(x) = x^2$ in inequation (54), immediately we have

$$\widetilde{\tau}_* \leq \widetilde{\tau} \leq \widetilde{\tau}_m, \quad (90)$$

which implies similarly that more concentrated mass leads to higher CE effect.

We now have some further discussion on the CE intensity factor. According to its definition, we infer that if $\tau < 1$, namely $R_\varepsilon > R_k$, which means the number of CEs is not sufficient enough to make the encountering distance approach the kinetic limitation, Trojan will not escape under the perturbation of Plutinos. Oppositely, if $\tau > 1$, the perturbation of Plutinos is prominent enough to influence the stability of Trojan. Hence $\tau = 1$ is a criterion for measuring the degree of interaction between two planetesimals and a larger τ implies a stronger interaction.

4. CONCLUSION

Back to the discussion in Paper I, we first recognize the randomness and unbiasedness lying in the close encounters (CEs) between Plutinos and Trojans, based on statistical analyses of pertinent variables associated with CE location. Meanwhile, the CE effects, which is our major concern, prove to distribute symmetrically on the positive and negative branch, indicating that the perturbations exerted by Plutinos probably have no effect on the inclination or eccentricity of Trojan.

Nevertheless, despite the symmetry, later explorations find that the tiny CE effect can continually accumulate to a prominent value through the random walk mechanism as long as there are sufficient number of CEs. The dependencies of the number of CEs and cumulative effect on the mass, inclination, eccentricity, libration amplitude of Plutino and Trojan are discussed seriatim, along with acceptable theoretical estimations. The even simplified analytical formula on CE effect can be put into practice conveniently. However, notwithstanding the random walk mechanism, the perturbations exerted by Plutinos are still hard to achieve a prominent effect, even with a completely exaggerated total mass, certainly less significant in consideration of the falling effect due to the dispersion of total mass over a vast quantity of planetesimals.

Rather interesting is the “knee” situated on the plot of cumulative effect concerning the mass of Plutino, which is later proved to result from the perturbation of Plutino becoming comparable to the force exerted by Neptune in a encounter particularly close, thus expelling Trojan from its resonant region. Obviously this mechanism can be triggered either by raising the mass of Plutino, thus directly enhancing the perturbation, or generating abundant CEs to bring about an encounter that is sufficiently close. It thereupon comes the inspiration that though Plutinos in reality is insufficiently massive to expel Trojan in the former way, they may take the

latter way by generating abundant CEs all together since the number of Plutinos in reality is tremendous. However, later calculations reveal that when more Plutinos share the total mass, the encountering distance required to kinetically influence Trojan shrinks more rapidly as mass of each Plutino drops, than the minimum encountering radius likely to be reached as the total number of CEs increases. Here we propose the CE intensity factor to measure the degree of perturbation exerted by a cluster of planetesimals on a specific body. The mono-concentrated case is proved to cause the largest effect, and for Plutinos with a exaggerated total mass of 10 Pluto mass, $\tau_m \approx 0.98$, which is quite close to the escaping threshold value 1, indicating a Plutino with 10 Pluto mass may have certain influence on Trojan. But for a more real case such as 10 Plutinos with Pluto mass each, $\tau \approx 0.31$, which is far from triggering the escaping mechanism.

To emphasize again, our theoretical analysis is completely based on the randomness of the close encounters. One may notice that we never mention the influence of other giant planets on our model apart from Neptune all along, which brings about the question that whether or not the perturbation of adjacent giant planets will break this randomness. In fact, the perturbation of giant planets will at most change the orbital characteristics of Plutino or Trojan over a long time scale, whereas it has been shown that the randomness of CEs

is satisfied within a broad range of orbital elements of Plutino and Trojan, and the interaction between planetesimals is a far more frequent activity.

It is inspiring that if we believe the close encounters to be a stochastic event in general cases, the theory we put forward above can be applied to the discussion on the interaction between two arbitrary groups of planetesimals. The number of CEs, the cumulative effect on the orbital elements and the probability to trigger the escape mechanism can all be immediately calculated through several simple formulas. And we have no need to worry about the great number of planetesimals likely to be encountered in the numerical simulation, as long as the total mass is determined and the mass distribution function is proposed.

Of course the Monte Carlo simulation and the mixed strategy serving as a modified substitute for the numerical simulation can be applied into other examples of planetesimal interactions as well. Under specific circumstances, they may be quite useful.

This work has been supported by the National Natural Science Foundation of China (NSFC, Grants No.11473016 & No.11333002).

REFERENCES

- Almeida, A. J. C., Peixinho, N., & Correia, A. C. M. 2009, *A&A*, 508, 1021
 Brasser, R., Mikkola, S., Huang, T.-Y., Wiegert, P., & Innanen, K. 2004, *MNRAS*, 347, 833
 Carruba, V., Roig, F., Michtchenko, T. A., Ferraz-Mello, S., & Nesvorný, D. 2007, *A&A*, 465, 315
 Dell’Oro, A., & Cellino, A. 2007, *MNRAS*, 380, 399
 Dong, C.-Y., & Zhou, L.-Y. 2017, submitted
 Dvorak, R., Lhotka, C., & Schwarz, R. 2008, *Celestial Mechanics and Dynamical Astronomy*, 102, 97
 Dvorak, R., Schwarz, R., Süli, Á., & Kotoulas, T. 2007, *MNRAS*, 382, 1324
 Greenberg, R. 1982, *AJ*, 87, 184
 Li, J., Zhou, L.-Y., & Sun, Y.-S. 2007, *A&A*, 464, 775
 Marzari, F., Tricarico, P., & Scholl, H. 2003, *MNRAS*, 345, 1091
 Pittichova, J. A., Meech, K. J., Wasserman, L. H., et al. 2003, *Minor Planet Electronic Circulars*, 2003
 Wetherill, G. W. 1967, *J. Geophys. Res.*, 72, 2429
 Zhou, L.-Y., Dvorak, R., & Sun, Y.-S. 2009, *MNRAS*, 398, 1217